Support of part of this work by the National Science Foundation (CHE7905897) and by the Centre National de la Recherche Scientifique under the US-France exchange program is gratefully acknowledged.

We are grateful to Drs Gregson and Howard for stimulating interactions during the course of this work.

References

BOSTON, J. L., SHARP, D. W. A. & WILKINSON, G. (1962). *J. Chem. Soc.* pp. 3488-3494.

CETINI, G., GAMBINO, O., ROSSETTI, R. & SAPPA, E. (1967). *J. Organomet. Chem.* pp. 149-154.

COPPENS, P., LEISEROWITZ, L. & RABINOVICH, D. (1965). *Acta Cryst.* **18**, 1035-1038.

GERMAIN, G., MAIN, P. & WOOLFSON, M. M. (1971). *Acta Cryst.* A**27**, 390-397.

GREGSON, D. & HOWARD, J. (1983). *Acta Cryst.* C**39**, 1024-1027.

HUHEEY, J. E. (1965). *J. Phys. Chem.* **69**, 3284-3291.

HUHEEY, J. E. (1978). *Principles of Structure and Reactivity*, pp. 563-671. New York: Harper International Edition.

International Tables for X-ray Crystallography (1974). Vol. IV. Birmingham: Kynoch Press.

ITTEL, J. E. & IBERS, J. A. (1976). *Adv. Organomet. Chem.* **14**, 33-35.

LEUNG, P. C. W. (1983). Thesis, State Univ. of New York at Buffalo.

LEUNG, P. C. W. & COPPENS, P. (1983). *Acta Cryst.* B**39**, 535-542.

STERNBERG, H. W., GREENFIELD, H., FRIEDEL, R. A., WOTIZ, J., MARKBY, R. & WENDER, I. (1954). *J. Am. Chem. Soc.* **76**, 1457-1458.

STEWART, R. F., DAVIDSON, E. R. & SIMPSON, W. T. (1965). *J. Chem. Phys.* **42**, 3175-3187.

THORN, D. L. & HOFFMANN, R. (1978). *Inorg. Chem.* **17**, 126-140.

Acta Cryst. (1984). B**40**, 595-606

Effect of Crystal Packing on Linkage Isomerism in the [Pd(1,1,7,7-tetraethyldiethylenetriamine)(thiocyanato)]$^+$ Cation: Structures of the Hexafluorophosphate Salt and of Four Crystal Forms of the Tetraphenylborate Salt

BY CAROLYN PRATT BROCK, JAMES L. HUCKABY AND THOMAS G. ATTIG*

Department of Chemistry, University of Kentucky, Lexington, Kentucky 40506-0055, *USA*

(*Received* 24 *February* 1984; *accepted* 30 *May* 1984)

Abstract

The influence of the counterion and crystal environment on the bonding mode of the ambidentate thiocyanate ion in the $[Pd(Et_4dien)CNS]^+$ cation (where Et_4dien is the 1,1,7,7-tetraethyldiethylenetriamine moiety, $Et_2NCH_2CH_2NHCH_2CH_2NEt_2$) has been investigated. It had been reported previously that the thiocyanate is N-bonded in the PF_6^- salt but that it undergoes an N- to S-bonded isomerization in the BPh_4^- salt. In crystals of the PF_6^- salt {$[Pd(NCS)(C_{12}H_{29}N_3)]PF_6$, $M_r = 524{\cdot}8$, orthorhombic, $P2_12_12_1$, $a = 11{\cdot}824\,(3)$, $b = 11{\cdot}838\,(2)$, $c = 15{\cdot}626\,(3)$ Å, $T = 296$ K, $Z = 4$, $V = 2187{\cdot}2$ Å^3, $D_x = 1{\cdot}594$ g cm^{-3}, $\mu = 10{\cdot}34$ cm^{-1}, Mo $K\alpha$, $\lambda = 0{\cdot}71069$ Å, $F(000) = 1060{\cdot}10$, 2500 observations with $I > 3\sigma(I)$, 300 variables, final R index on F_o of 0·033} the thiocyanate is N-bonded as expected. It is, however, also N-bonded in two stable crystal forms of the BPh_4^- salt {acetone solvate: $[Pd(NCS)(C_{12}H_{29}N_3)][B(C_6H_5)_4].C_3H_6O$, $M_r = 757{\cdot}2$, monoclinic, $P2_1/c$, $a = 11{\cdot}927\,(2)$, $b = 19{\cdot}250\,(3)$, $c = 17{\cdot}252\,(3)$ Å, $\beta = 100{\cdot}33\,(2)°$, $T = 143$ K, $Z = 4$, $V = 3896{\cdot}8$ Å^3, $D_x = 1{\cdot}291$ g cm^{-3}, μ(Mo $K\alpha$) = 5·54 cm^{-1}, $F(000) = 1587{\cdot}74$, 5221 observations with $I > 3\sigma(I)$, 265 variables, final R on F_o of 0·044} {unsolvated: $[Pd(NCS)(C_{12}H_{29}N_3)][B(C_6H_5)_4]$, $M_r = 699{\cdot}1$, orthorhombic, $P2_12_12_1$, $a = 9{\cdot}566\,(2)$, $b = 14{\cdot}745\,(5)$, $c = 24{\cdot}419\,(7)$ Å, $T = 150$ K, $Z = 4$, $V = 3444{\cdot}3$ Å^3, $D_x = 1{\cdot}348$ g cm^{-3}, μ(Mo $K\alpha$) = 6·19 cm^{-1}, $F(000) = 1459{\cdot}74$, 5144 observations with $I > 3\sigma(I)$, 229 variables, final R on F_o of 0·045}. A third crystal form {CH_2BrCl solvate: $[Pd(NCS)(C_{12}H_{29}N_3)][B(C_6H_5)_4].CH_2BrCl$, $M_r = 828{\cdot}5$, monoclinic, $P2_1/n$, $a = 11{\cdot}058\,(3)$, $b = 20{\cdot}833\,(10)$, $c = 16{\cdot}955\,(5)$ Å, $\beta = 100{\cdot}72\,(3)°$, $T = 150$ K, $Z = 4$, $V = 3837{\cdot}8$ Å^3, $D_x = 1{\cdot}434$ g cm^{-3}, μ(Mo $K\alpha$) = 16·62 cm^{-1}, $F(000) = 1698{\cdot}83$, 4940 observations with $I > 3\sigma(I)$, 256 variables, final R on F_o of 0·045} loses solvent but does not isomerize. A fourth crystal form of the BPh_4^- salt is S-bonded but unstable {CH_3OH solvate: $[Pd(SCN)(C_{12}H_{29}N_3)][B(C_6H_5)_4].CH_4O$, $M_r = 731{\cdot}1$, monoclinic, $P2_1/n$ or $P2_1$, $a = 12{\cdot}748\,(5)$, $b = 9{\cdot}929\,(3)$, $c = 29{\cdot}112\,(18)$ Å, $\beta = 97{\cdot}39\,(6)°$, $T = 137$ K, $Z = 4$, $V = 3654{\cdot}2$ Å^3, $D_x = 1{\cdot}329$ g cm^{-3}, μ(Mo $K\alpha$) = 5·88 cm^{-1}, $F(000) = 1531{\cdot}74$, 1346 observations with $I > 3\sigma(I)$, 174 variables, final R on F_o of 0·050}. In this last crystal form the N end of the S-bonded ligand is hydrogen-bonded to the incorporated solvent. Other crystal forms were discovered but not investigated in detail. Some packing

* Present address: Standard Oil Company of Ohio, 9101 East Pleasant Valley Road, Independence, Ohio 44131, USA.

0108-7681/84/060595-12$01.50

motifs common to the five crystal structures are described, and a method for assessing relative density of packing based on crystallographic thermal parameters is suggested. Variations between the geometries of the N-bonded cation in its four crystal environments are discussed. It is concluded that stabilization of the S-bonded isomer of the [Pd(1,1,7,7-tetraethyldiethylenetriamine)(thiocyanato)]$^+$ cation in specific crystalline modifications of $B(C_6H_5)_4^-$ salts should be ascribed to the crystal packing in those particular structures rather than to the nature of the non-coordinating counterion.

Introduction

Many factors influence the bonding mode of the ambidentate thiocyanate ligand. The contributions to a preference for *M*-SCN or *M*-NCS* bonding of the metal, the steric properties of *cis* ligands, the electronic properties of ancillary ligands, and of the solvent have been discussed extensively (Burmeister, 1975; Norbury, 1975; MacDougall, Nelson, Fultz, Burmeister, Holt & Alcock, 1982, and references therein), and it is clear that the balance of factors favoring one or the other isomer is very subtle. Early on it was also reported (Burmeister, Gysling & Lim, 1969; hereafter, BGL) that the bonding mode of the thiocyanate ligand may be influenced by the specific nature of a non-coordinating counterion. The compound $[Pd(Et_4dien)CNS]X$ (where Et_4dien is the 1,1,7,7-tetraethyldiethylenetriamine moiety,† Et_2N-$CH_2CH_2NHCH_2CH_2NEt_2$) was found (BGL, 1969) to be N-bonded for $X = PF_6^-$ but to undergo N- to S-bonded isomerization in the solid state when $X = BPh_4^-$. This isomerization was studied further using infrared spectroscopy (Lauer, Peterkin, Burmeister, Johnson & Lim, 1972), and an explanation was proposed (Burmeister, Hassel, Johnson & Lim, 1974) based on crystal-packing requirements although no structural work had been done.

We became interested in this problem after encountering another system (Brock & Attig, 1980) in which a linkage isomerization (the $\eta^1 \rightarrow \eta^3$ rearrangement of a Pt-allyl cation) occurs upon crystallization when the non-coordinating counterion is changed from BPh_4^- to PF_6^-. We therefore began studying salts of the $[Pd(Et_4dien)CNS]^+$ cation in order to extend our understanding of the influence of these two counterions. Instead, we found the solid-state chemistry of the BPh_4^- salt to be much more complicated than suspected, and its reported isomerization to be elusive.

* Throughout this paper metal-thiocyanate and metal-isothiocyanate bonding are designated by *M*-SCN and *M*-NCS respectively. We also make use of the convention (somewhat reluctantly, since there is no *M*-C bond) that *M*-CNS represents cases for which the point of attachment of the ligand is unspecified.

† Alternative nomenclature: 3,9-diethyl-3,6,9-triazaundecane.

Experimental

Characterization of crystal forms

The PF_6^- (Basolo, Baddley & Weidenbaum, 1966) and BPh_4^- (BGL, 1969) salts of the $[Pd(Et_4dien)CNS]^+$ cation were synthesized following procedures in the literature. Crystals of the PF_6^- salt (1) suitable for an X-ray diffraction study were obtained by slow evaporation of an acetone solution. Trial recrystallizations of the BPh_4^- salt from several solvents, however, gave a bewildering variety of crystal forms. These were characterized by examining their morphologies under a microscope, determining the unit-cell parameters with a CAD-4/F X-ray diffractometer, and indexing the crystal faces observed with an optical goniometer. Zero- and several upper-level Weissenberg photographs were also taken for all the stable crystals. Details for some of the crystal forms are given in the *Abstract* and in Table 1. All work was performed at room temperature unless otherwise stated.

Evaporation of an acetone solution of the BPh_4^- salt yields chunky, multifaceted crystals (2) which proved to be an acetone solvate of the N-bonded isomer. These crystals also grow as needles elongated along **c** and as lozenges with large {001} faces, and also precipitate from mixtures of acetone and methanol or ethanol. These crystals exhibit no signs of instability.

Evaporation of acetone/CH_3OH solutions of the BPh_4^- salt also yields two other crystal forms. One, (3), which contains the N-bonded isomer, grows as thick needles or prisms without the incorporation of solvent. Being particularly interested in the stability of this pure material to isomerization, we grew a very large ($6 \times 4 \times 2$ mm) crystal of this type over a period of 30 d, used two parts of it to take infrared spectra 22 weeks apart, and mounted the remainder on a Weissenberg camera. Films confirmed that the crystal was the same as the unsolvated BPh_4^- salt mounted on the diffractometer; the infrared spectrum did not change with time. The other crystal form (4) also grows as prisms but of a slightly different shape and in clusters. Films, diffractometer and goniometer measurements show that these latter crystals are monoclinic, with $a = 10{\cdot}356\,(13)$, $b = 12{\cdot}236\,(6)$, $c = 28{\cdot}814\,(13)$ Å, and $\beta = 90{\cdot}28\,(8)°$ and are bounded by planes of the forms {001}, {01$\bar{1}$}, and {012}. There is no glide plane, and no evidence in the films for decomposition with time, although cracks do develop perpendicular to the length of the crystals. The diffracted peaks are quite wide and difficult to center, and intensity data were not collected.

Still attempting to grow crystals of the S-bonded isomer, we tried more elaborate recrystallizations. Methanol, in which the BPh_4^- salt is very insoluble, was carefully layered over a saturated CH_2Cl_2 solution in a test tube and allowed to sit for several days

Table 1. *Additional crystal data and details of intensity collection and refinement*

Structure designation	(1)	(2)	(3)	(5)	(7)
Anion; solvent	PF_6^-	BPh_4^-; $(CH_3)_2CO$	BPh_4^-	BPh_4^-; CH_2BrCl	BPh_4^-; CH_3OH
Formula	$C_{13}H_{29}F_6N_4PPdS$	$C_{40}H_{55}BN_4OPdS$	$C_{37}H_{49}BN_4PdS$	$C_{38}H_{51}BBrClN_4PdS$	$C_{38}H_{53}BN_4OPdS$
Morphology	Prisms	Chunks (also needles and plates)	Prisms	Needles	Plates
Bounding planes	{011}, {111}, {110}	{010}, {011}, {110}	{100}, {001}, {011}		
Radiation	Mo $K\alpha$; graphite monochromator				
Crystal size (mm)	0·35×0·30×0·26	0·51×0·36×0·26	0·36×0·22×0·19	0·25×0·20×0·10	
Transmission factors	0·816–0·852		0·897–0·905		
Decomposition (%)	2·4	2·0	4·7	4·6	11·2
Take-off angle (°)	1·9	2·4	2·1	2·4	2·0
Scan angle (°)*	0·90	0·80	0·80	0·80	0·80
Max. scan time (s)†	120	80	80	90	80
Target signal/noise ratio	50:1	50:1	100:1	20:1	100:1
Max. 2θ (°)	60·0 (0·704 Å^{-1})	50·0 (0·595 Å^{-1})	60·0 (0·704 Å^{-1})	50·0 (0·595 Å^{-1})	30·0 (0·364 Å^{-1})
Data collected	$+h, +k, +l$	$+h, +k, \pm l$	$+h, +k, +l$	$\pm h, +k, +l$	$\pm h, +k, +l$
p factor‡	0·04	0·03	0·03	0·04	0·04
Unique data	3563	6835	5578	6571	1469 (1622 in $P2_1$)
Unique data with $F_o^2 > 3\sigma(F_o^2)$	2500	5221	5144	4940	1346 (1360 in $P2_1$)
Final number of variables	300	265	229	256	174
R, R_w on F ($>3\sigma$)	3·3, 3·9	4·4, 6·0	4·5, 6·1	4·5, 6·2	5·0, 6·9
Error in observation of unit weight (e)	1·27	2·63	2·69	1·81	3·08
Highest peak in final difference Fourier (e Å^{-3})	0·32	1·38	1·27	1·14	0·62
C–N asymmetric stretch (cm^{-1})	2100	2089	2100	2090	2131, 2113§
Isomer	NCS^-	NCS^-	NCS^-	NCS^-	SCN^-

* 2θ angle scanned ($\theta/2\theta$) each side of $K\alpha$ doublet to obtain integrated peak intensity; scan extended an additional 25% at each end for backgrounds.

† Scan time depends on intensity found during a prescan.

‡ See Brock & Webster (1976).

§ Measured for room-temperature form (6) which has a different unit cell, twice as large. With time the 2131 cm^{-1} band decreases and the 2113 cm^{-1} band increases in intensity (see text).

at 258 K. Crystals formed both at the interface of the solvent layers and at the bottom of the test tube. In order to lengthen the time the crystals grew at the interface before sinking, the denser solvents CH_2BrCl and CH_2Br_2 were also tried. The crystals that grow at the bottom (5) contain N-bonded cations and the dihalomethane solvent. At room temperature these crystals usually lose solvent and become microcrystalline within hours, but the NCS^- bands of the infrared spectrum are unaffected. At low temperature the crystals are stable.

A time-dependent infrared spectrum was observed for the crystals that grow at the solvent-layer interface as plates. At room temperature the crystals appear to be monoclinic (space group probably $P2_1/c$) (6) with $a = 18{\cdot}0$, $b = 13{\cdot}0$, $c = 30{\cdot}4$ Å, and $\beta = 94{\cdot}°$, and are bounded by faces of the forms {100}, {111}, and {10$\bar{2}$}. They are unstable, and the cell constants vary significantly with time and between crystals. Crystals grown over several days at the solvent-layer interface and mounted immediately at low temperatures (7) are more stable, but have a different unit cell, approximately half as large as the room-temperature cell. A subsequent structure determination showed that these latter crystals contain S-bonded cations.

Some other, probably different, crystals were observed which were either too small or too unstable to be studied crystallographically. Some of these, when observed under the polarizing microscope, appeared to undergo very slow transformations starting at one corner or end of the crystals and during which crystallinity was preserved. Months were required for even partial transformation.

Crystal structure determinations

Crystals were mounted on fibers in air and immediately transferred to an Enraf–Nonius CAD-4/F diffractometer equipped (except in the case of the PF_6^- salt) with an LT-1 low-temperature device operating at or just below 150 K. Procedures and programs described previously (Brock & Webster, 1976) were utilized during data collection, structure solution (heavy-atom methods), and refinement; details are summarized in Table 1. Anomalous terms were included for Pd, Br, Cl, S, and P atoms. The H atoms, which were readily located in difference maps, were included as fixed contributions after idealization. Absorption corrections were made for two of the structures, but cost-benefit considerations

Table 2. *Positional and thermal parameters for the atoms of* (1)

Estimated standard deviations in the least significant figure(s) are given in parentheses in this and all subsequent tables. The equivalent B's are calculated from the anisotropic thermal parameters β and the direct metric $\mathbf{G}$ as $\frac{4}{3}\mathrm{Tr}(\boldsymbol{\beta}.\mathbf{G})$.

	x	y	z	B_{eq}(Å^2)		x	y	z	B_{eq}(Å^2)
Pd	0·03584 (3)	0·03586 (3)	0·10750 (3)	3·8	N(2)	0·0000 (4)	−0·1265 (4)	0·0855 (3)	4·1
S	0·1065 (2)	0·42897 (15)	0·14477 (16)	8·2	N(3)	−0·1297 (4)	0·0676 (4)	0·0655 (3)	4·7
P	0·04516 (16)	−0·25535 (15)	−0·14271 (11)	5·5	C(NCS)	0·0850 (5)	0·2958 (5)	0·1328 (4)	4·7
F(1)	−0·0287 (13)	−0·3280 (13)	−0·2039 (11)	9·6	C(1)	0·1866 (5)	−0·1498 (5)	0·1389 (4)	4·9
F(2)	0·108 (2)	−0·166 (2)	−0·0856 (9)	12·5	C(2)	0·0698 (5)	−0·1961 (5)	0·1444 (4)	5·3
F(3)	0·1559 (9)	−0·297 (2)	−0·1821 (11)	12·0	C(3)	−0·1263 (5)	−0·1398 (5)	0·0898 (4)	4·8
F(4)	0·0455 (15)	−0·1619 (13)	−0·2165 (11)	11·3	C(4)	−0·1751 (4)	−0·0448 (6)	0·0363 (4)	5·0
F(5)	−0·0675 (10)	−0·2148 (18)	−0·1043 (13)	12·2	C(5)	0·1791 (6)	−0·0092 (8)	0·2552 (5)	7·0
F(6)	0·042 (2)	−0·3410 (16)	−0·0735 (11)	15·8	C(6)	0·2712 (14)	−0·0514 (13)	0·3046 (7)	8·6
F(1′)	−0·0462 (17)	−0·289 (2)	−0·0695 (10)	8·8	C(6′)	0·140 (2)	0·083 (2)	0·2979 (12)	8·0
F(2′)	0·133 (3)	−0·224 (2)	−0·2071 (16)	15·0	C(7)	0·2932 (5)	0·0285 (7)	0·1264 (5)	6·1
F(3′)	0·1277 (12)	−0·241 (2)	−0·0597 (15)	10·8	C(8)	0·2996 (7)	0·0347 (8)	0·0309 (5)	7·3
F(4′)	0·025 (3)	−0·1323 (13)	−0·122 (2)	15·8	C(9)	−0·1961 (6)	0·1072 (7)	0·1440 (5)	6·6
F(5′)	−0·038 (2)	−0·282 (3)	−0·2126 (15)	14·8	C(10)	−0·3145 (7)	0·1345 (9)	0·1290 (8)	9·6
F(6′)	0·079 (2)	−0·3816 (12)	−0·1438 (15)	12·7	C(11)	−0·1352 (6)	0·1534 (6)	−0·0041 (5)	6·2
N(NCS)	0·0718 (4)	0·2005 (4)	0·1277 (4)	5·6	C(12)	−0·0549 (8)	0·1333 (7)	−0·0766 (5)	7·6
N(1)	0·1854 (4)	−0·0258 (5)	0·1592 (3)	4·6					

Table 3. *Positional and thermal parameters for the non-group atoms of* (2)

The equivalent B's are calculated from the anisotropic thermal parameters β and the direct metric $\mathbf{G}$ as $\frac{4}{3}\mathrm{Tr}(\boldsymbol{\beta}.\mathbf{G})$.

	x	y	z	B_{eq}(Å^2)		x	y	z	B_{eq}(Å^2)
Pd	0·25029 (3)	0·011482 (16)	0·287845 (18)	2·7	C(5)	0·2418 (5)	−0·0712 (3)	0·1498 (3)	4·8
S	0·20876 (15)	−0·21689 (7)	0·37864 (10)	6·1	C(6)	0·2728 (6)	−0·0994 (3)	0·0769 (3)	6·1
O(SOL)	0·4718 (3)	0·1409 (2)	0·3325 (3)	6·8	C(7)	0·4360 (5)	−0·0710 (2)	0·2322 (3)	4·2
N(NCS)	0·2399 (4)	−0·0816 (2)	0·3400 (2)	3·9	C(8)	0·5154 (4)	−0·0390 (3)	0·3008 (3)	4·8
N(1)	0·3326 (3)	−0·02822 (18)	0·2023 (2)	3·3	C(9)	0·0322 (4)	0·0304 (2)	0·3320 (3)	3·7
N(2)	0·2587 (3)	0·10350 (17)	0·2352 (2)	3·3	C(10)	−0·0603 (5)	0·0587 (3)	0·3741 (3)	5·1
N(3)	0·1489 (3)	0·06221 (18)	0·3556 (2)	3·4	C(11)	0·1887 (5)	0·0544 (3)	0·4429 (3)	4·9
C(NCS)	0·2272 (4)	−0·1356 (3)	0·3554 (2)	3·1	C(12)	0·3153 (5)	0·0651 (3)	0·4684 (3)	5·4
C(1)	0·3653 (4)	0·0334 (3)	0·1581 (3)	3·9	C(S1)	0·6156 (6)	0·2150 (5)	0·3255 (6)	9·9
C(2)	0·2760 (4)	0·0898 (2)	0·1533 (3)	4·1	C(S2)	0·5636 (4)	0·1585 (3)	0·3600 (4)	5·1
C(3)	0·1574 (4)	0·1436 (2)	0·2457 (3)	4·3	C(S3)	0·6312 (5)	0·1249 (4)	0·4341 (5)	7·6
C(4)	0·1491 (4)	0·1374 (2)	0·3312 (3)	4·4	B	0·2142 (4)	0·1303 (2)	0·8665 (3)	2·3

precluded correcting the other three data sets. In no case did extinction appear important, nor did analyses of $\sum w(|F_o|-|F_c|)^2$ [where $w=4F_o^2/\sigma^2(F_o^2)$] as a function of $|F_o|$, $\sin\theta/\lambda$, or the Miller indices reveal any important trends. The highest peaks in the final difference maps (see Table 1) are associated with the heavy atoms, the PF_6^- ions, and, especially, the phenyl rings. The final coordinates and equivalent B's of the atoms and the derived positions of the BPh_4^- ring C atoms and rigid-body parameters for the five structures are listed in Tables 2–10. The atom-numbering scheme for the cation, which is the same for all the structures, is shown in Fig. 1(*a*). Some bond lengths and angles, which are in good agreement with those known for related structures (Nelson, MacDougall, Alcock & Mathey, 1982) are shown in Fig. 1.* Additional comments on two of the individual structure determinations are given below.

PF_6^- *salt* (1). Difference maps late in the refinement showed that C(6) is unequally distributed [occupancy factor for C(6)′ is 0·385 (16)] between two positions. Even after inclusion of the disorder in the model, standard deviations, thermal parameters, and bond lengths indicate that the affected ethyl group is not described very precisely. The F atoms of the anion are also disordered between at least two positions [occupancy factors for F(1) through F(6) are 0·573 (18)].

BPh_4^- *salt*; CH_3OH *solvate* (7). This structure presented numerous crystallographic problems. The crystals are slow-growing but unstable, so that it was difficult to choose an optimum time for harvesting and transferring the rather thin plates to the cold stream on the diffractometer. The long c axis caused some overlap problems, and there were some difficulties with the low-temperature system. After collecting data on three crystals we finally settled for a very limited data set with the understanding that the structure would not be determined very precisely.

The space group is ambiguous. The $h0l$, $h+l$ odd reflections are very weak, but 14 of 152 collected have $I>3\sigma(I)$. The structure was solved in $P2_1/n$, but the rings of the BPh_4^- anion are disordered by an approximate mirror plane perpendicular to **b** that passes through the B atom. Furthermore, the occupancy factors for the two orientations do not differ significantly from $\frac{1}{2}$, and packing considerations [see Fig. 2(*e*)] show that neighboring anions cannot be related by an n glide or a center of symmetry (at least

* Lists of structure factors, anisotropic thermal parameters and parameters of the fixed atoms have been deposited with the British Library Lending Division as Supplementary Publication No. SUP 39501 (138 pp.). Copies may be obtained through The Executive Secretary, International Union of Crystallography, 5 Abbey Square, Chester CH1 2HU, England.

Table 4. *Derived parameters for the rigid-group atoms of* (2)

	x	y	z	B (Å^2)		x	y	z	B (Å^2)
*R*1C1	0·1795 (2)	0·04529 (10)	0·86652 (16)	2·50 (7)	*R*3C1	0·10487 (18)	0·17710 (14)	0·88900 (13)	2·32 (7)
*R*1C2	0·2401 (2)	−0·00226 (13)	0·82886 (16)	3·28 (8)	*R*3C2	0·0158 (2)	0·19943 (14)	0·83038 (11)	2·89 (7)
*R*1C3	0·2161 (2)	−0·07317 (12)	0·83127 (17)	3·60 (9)	*R*3C3	−0·0759 (2)	0·23591 (15)	0·85085 (14)	3·49 (8)
*R*1C4	0·1314 (2)	−0·09652 (10)	0·87135 (18)	3·75 (9)	*R*3C4	−0·0785 (2)	0·25006 (15)	0·92993 (16)	3·65 (9)
*R*1C5	0·0707 (2)	−0·04897 (13)	0·90901 (17)	3·65 (9)	*R*3C5	0·0107 (2)	0·22774 (15)	0·98855 (11)	3·42 (8)
*R*1C6	0·0948 (2)	0·02193 (12)	0·90660 (16)	2·95 (7)	*R*3C6	0·1023 (2)	0·19126 (14)	0·96809 (12)	2·95 (8)
*R*2C1	0·2364 (2)	0·15183 (14)	0·77569 (12)	2·42 (7)	*R*4C1	0·33266 (18)	0·14554 (12)	0·93337 (14)	2·30 (7)
*R*2C2	0·3258 (2)	0·19496 (14)	0·76360 (13)	2·78 (7)	*R*4C2	0·3603 (2)	0·21422 (10)	0·95495 (15)	2·92 (8)
*R*2C3	0·3357 (2)	0·21490 (14)	0·68726 (15)	3·36 (8)	*R*4C3	0·4589 (2)	0·22881 (10)	1·00958 (16)	3·31 (8)
*R*2C4	0·2561 (2)	0·19172 (16)	0·62301 (12)	3·87 (9)	*R*4C4	0·5298 (2)	0·17471 (14)	1·04263 (15)	3·48 (8)
*R*2C5	0·1666 (2)	0·14859 (16)	0·63510 (13)	3·93 (9)	*R*4C5	0·5021 (2)	0·10603 (12)	1·02105 (16)	3·77 (9)
*R*2C6	0·1568 (2)	0·12865 (14)	0·71144 (15)	3·27 (8)	*R*4C6	0·4036 (2)	0·09144 (9)	0·96642 (16)	2·93 (8)

Rigid-group parameters

Group	x_c*	y_c	z_c	δ†	ε	η
Ring 1	0·15544 (16)	−0·02562 (9)	0·86894 (11)	1·3042 (18)	−2·3899 (18)	3·050 (2)
Ring 2	0·24624 (15)	0·17178 (9)	0·69935 (11)	2·1425 (18)	2·9173 (13)	−1·3836 (18)
Ring 3	0·01320 (15)	0·21358 (9)	0·90947 (11)	−1·724 (4)	−2·0095 (14)	1·959 (4)
Ring 4	0·43122 (15)	0·16012 (9)	0·98800 (10)	−2·9302 (14)	−3·0980 (17)	2·5898 (17)

* x_c, y_c, and z_c are the fractional coordinates of the origin of the rigid group.
† The rigid-group orientation angles δ, ε, and η (radians) have been defined previously (La Placa & Ibers, 1965).

Table 5. *Positional and thermal parameters for the non-group atoms of* (3)

The equivalent B's are calculated from the anisotropic thermal parameters β and the direct metric $\mathbf{G}$ as $\frac{4}{3}$ Tr (β.$\mathbf{G}$).

	x	y	z	B_{eq}(Å^2)		x	y	z	B_{eq}(Å^2)
Pd	0·04976 (4)	0·10509 (2)	0·048406 (13)	1·6	C(4)	0·0832 (6)	0·1151 (4)	0·16561 (19)	2·7
S	0·13661 (19)	0·37138 (10)	−0·05490 (8)	4·3	C(5)	0·1100 (5)	−0·0290 (3)	−0·0387 (2)	2·3
N(NCS)	0·1075 (5)	0·2064 (3)	−0·00135 (18)	2·5	C(6)	0·2097 (7)	0·0326 (4)	−0·0682 (3)	3·4
N(1)	−0·0150 (4)	0·0152 (3)	−0·01192 (16)	2·0	C(7)	−0·1065 (6)	0·0613 (4)	−0·0542 (2)	2·6
N(2)	−0·0199 (5)	0·0115 (3)	0·10096 (18)	2·4	C(8)	−0·1635 (8)	−0·0013 (4)	−0·0993 (3)	3·7
N(3)	0·1299 (4)	0·1698 (3)	0·11722 (16)	1·9	C(9)	0·2870 (6)	0·1652 (4)	0·1108 (2)	2·6
C(NCS)	0·1190 (6)	0·2747 (3)	−0·0230 (2)	2·2	C(10)	0·3725 (7)	0·2128 (5)	0·1559 (2)	3·8
C(1)	−0·0957 (6)	−0·0571 (3)	0·0177 (2)	2·6	C(11)	0·0866 (6)	0·2663 (3)	0·1241 (2)	2·5
C(2)	−0·0320 (6)	−0·0769 (3)	0·0727 (2)	2·6	C(12)	−0·0670 (7)	0·2827 (4)	0·1129 (3)	3·3
C(3)	0·0730 (6)	0·0157 (4)	0.1502 (2)	2·7	B	0·4019 (5)	0·3025 (3)	0·34514 (19)	1·4

Table 6. *Derived parameters for the rigid-group atoms of* (3)

	x	y	z	B (Å^2)		x	y	z	B (Å^2)
*R*1C1	0·3250 (3)	0·20372 (15)	0·32857 (12)	1·62 (7)	*R*3C1	0·3150 (3)	0·39067 (16)	0·31535 (11)	1·70 (6)
*R*1C2	0·1817 (3)	0·19239 (17)	0·33735 (13)	2·10 (7)	*R*3C2	0·2312 (3)	0·37557 (15)	0·26938 (12)	1·90 (7)
*R*1C3	0·1164 (2)	0·1115 (2)	0·32212 (14)	2·22 (7)	*R*3C3	0·1800 (3)	0·4490 (2)	0·23931 (11)	2·30 (8)
*R*1C4	0·1943 (3)	0·04191 (16)	0·29812 (13)	2·26 (8)	*R*3C4	0·2125 (4)	0·53754 (16)	0·25521 (13)	2·52 (8)
*R*1C5	0·3376 (3)	0·05324 (17)	0·28934 (13)	2·35 (8)	*R*3C5	0·2963 (4)	0·55264 (14)	0·30118 (13)	2·64 (9)
*R*1C6	0·4029 (2)	0·1342 (2)	0·30456 (13)	1·95 (7)	*R*3C6	0·3475 (3)	0·4792 (2)	0·33125 (11)	2·11 (7)
*R*2C1	0·4076 (4)	0·3151 (2)	0·41390 (10)	1·93 (7)	*R*4C1	0·5641 (3)	0·3018 (2)	0·31906 (12)	1·77 (7)
*R*2C2	0·3276 (3)	0.2607 (2)	0·44872 (13)	2·41 (8)	*R*4C2	0·5840 (3)	0·3245 (2)	0·25406 (11)	2·18 (8)
*R*2C3	0·3378 (4)	0·2714 (2)	0·50542 (12)	3·37 (11)	*R*4C3	0·7169 (3)	0·3182 (3)	0·24073 (10)	2·94 (9)
*R*2C4	0·4280 (4)	0·3366 (3)	0·52730 (10)	3·71 (11)	*R*4C4	0·8301 (3)	0·2892 (3)	0·27241 (14)	3·21 (10)
*R*2C5	0·5079 (4)	0·3910 (2)	0·49248 (14)	3·79 (11)	*R*4C5	0·8102 (3)	0·2666 (3)	0·32741 (14)	3·14 (10)
*R*2C6	0·4977 (4)	0·3802 (2)	0·43578 (13)	2·78 (9)	*R*4C6	0·6772 (3)	0·2729 (2)	0·35074 (10)	2·87 (9)

Rigid-group parameters

Group	x_c*	y_c	z_c	δ†	ε	η
Ring 1	0·3250 (3)	0·20372 (15)	0·32857 (12)	0·0543 (16)	−2·7346 (19)	2·974 (2)
Ring 2	0·4076 (4)	0·3151 (2)	0·41390 (10)	2·433 (4)	2·2258 (18)	1·529 (4)
Ring 3	0·3150 (3)	0·39067 (16)	0·31535 (11)	−3·067 (2)	−2·9981 (17)	−0·947 (2)
Ring 4	0·5641 (3)	0·3018 (2)	0·31906 (12)	1·354 (2)	3·0573 (17)	−1·305 (2)

* x_c, y_c, and z_c are the fractional coordinates of the origin of the rigid group.
† The rigid-group orientation angles δ, ε, and η (radians) have been defined previously (La Placa & Ibers, 1965).

Table 7. *Positional and thermal parameters for the non-group atoms of* (5)

The equivalent B's are calculated from the anisotropic thermal parameters β and the direct metric $\mathbf{G}$ as $\frac{4}{3}$ Tr (β.$\mathbf{G}$).

	x	y	z	B_{eq}(Å^2)		x	y	z	B_{eq}(Å^2)
Pd	0·31731 (3)	0·084206 (17)	0·31133 (2)	1·5	C(4)	0·3423 (5)	0·2005 (2)	0·4067 (3)	2·5
Br	0·84938 (7)	0·04556 (4)	0·45650 (4)	4·7	C(5)	0·1893 (4)	0·0440 (2)	0·1577 (3)	1·9
Cl	0·80609 (18)	−0·07813 (9)	0·35646 (10)	4·8	C(6)	0·1647 (5)	0·0172 (3)	0·0724 (3)	2·8
S	0·16263 (17)	−0·12400 (8)	0·34591 (14)	5·1	C(7)	0·3922 (5)	−0·0091 (3)	0·1924 (3)	2·5
N(NCS)	0·2556 (4)	−0·0009 (2)	0·3461 (2)	2·3	C(8)	0·5127 (5)	−0·0128 (3)	0·2511 (3)	3·0
N(1)	0·3218 (3)	0·05253 (19)	0·1961 (2)	1·7	C(9)	0·1699 (5)	0·1289 (3)	0·4280 (3)	2·8
N(2)	0·3775 (3)	0·16817 (19)	0·2757 (2)	1·8	C(10)	0·0736 (5)	0·1492 (3)	0·3570 (4)	3·3
N(3)	0·3010 (4)	0·1313 (2)	0·4159 (2)	1·9	C(11)	0·3804 (5)	0·1017 (3)	0·4890 (3)	2·4
C(NCS)	0·2177 (5)	−0·0518 (3)	0·3452 (3)	2·5	C(12)	0·5125 (5)	0·0894 (3)	0·4807 (3)	3·2
C(1)	0·3811 (5)	0·1062 (3)	0·1564 (3)	2·2	C(SOL)	0·8892 (7)	−0·0057 (4)	0·3695 (4)	4·6
C(2)	0·3440 (5)	0·1705 (2)	0·1867 (3)	2·2	B	0·7437 (5)	0·1548 (3)	0·0915 (3)	1·6
C(3)	0·3247 (5)	0·2199 (2)	0·3196 (3)	2·2					

Table 8. *Derived parameters for the rigid-group atoms of* (5)

	x	y	z	B (Å^2)		x	y	z	B (Å^2)
*R*1C1	0·7022 (3)	0·18771 (14)	0·17476 (15)	1·90 (8)	*R*3C1	0·7536 (3)	0·07427 (10)	0·10267 (19)	1·68 (8)
*R*1C2	0·7183 (3)	0·15284 (11)	0·24633 (18)	2·20 (9)	*R*3C2	0·8618 (2)	0·04711 (13)	0·14528 (18)	2·10 (9)
*R*1C3	0·6890 (3)	0·18065 (14)	0·31534 (14)	2·63 (10)	*R*3C3	0·8683 (2)	−0·01898 (13)	0·15937 (19)	2·21 (9)
*R*1C4	0·6435 (3)	0·24333 (15)	0·31280 (15)	2·67 (10)	*R*3C4	0·7668 (3)	−0·05791 (10)	0·1308 (2)	2·13 (9)
*R*1C5	0·6275 (3)	0·27821 (12)	0·24124 (19)	2·60 (9)	*R*3C5	0·6586 (2)	−0·03075 (12)	0·08822 (19)	2·17 (9)
*R*1C6	0·6568 (3)	0·25040 (14)	0·17222 (15)	2·51 (9)	*R*3C6	0·6520 (2)	0·03534 (13)	0·07413 (18)	1·79 (8)
*R*2C1	0·6375 (2)	0·17147 (16)	0·00595 (14)	1·82 (8)	*R*4C1	0·8845 (2)	0·18530 (14)	0·08202 (19)	1·80 (8)
*R*2C2	0·5195 (3)	0·19298 (17)	0·01104 (14)	2·30 (9)	*R*4C2	0·9503 (3)	0·15507 (12)	0·02975 (18)	2·12 (9)
*R*2C3	0·4322 (2)	0·20270 (17)	−0·05885 (19)	2·82 (10)	*R*4C3	1·0609 (3)	0·18146 (15)	0·01647 (19)	2·48 (9)
*R*2C4	0·4629 (2)	0·19091 (17)	−0·13382 (15)	2·59 (9)	*R*4C4	1·1057 (2)	0·23807 (15)	0·0555 (2)	2·71 (10)
*R*2C5	0·5809 (3)	0·16940 (17)	−0·13891 (13)	2·48 (9)	*R*4C5	1·0399 (3)	0·26829 (13)	0·1077 (2)	2·62 (10)
*R*2C6	0·6682 (2)	0·15968 (16)	−0·06902 (17)	2·20 (9)	*R*4C6	0·9293 (3)	0·24191 (14)	0·12101 (18)	2·16 (9)

Rigid-group parameters

Group	x_c^*	y_c	z_c	δ†	ε	η
Ring 1	0·6729 (2)	0·21552 (10)	0·24378 (13)	0·318 (2)	2·6557 (15)	1·658 (2)
Ring 2	0·55021 (19)	0·18119 (10)	−0·06394 (12)	−1·977 (3)	2·3838 (15)	−1·436 (3)
Ring 3	0·76018 (18)	0·00818 (10)	0·11675 (11)	1·6779 (16)	2·816 (2)	2·971 (2)
Ring 4	0·99512 (19)	0·21168 (10)	0·06874 (12)	0·126 (2)	−2·424 (2)	−0·444 (3)

* x_c, y_c, and z_c are the fractional coordinates of the origin of the rigid group.
† The rigid-group orientation angles δ, ε, and η (radians) have been defined previously (La Placa & Ibers, 1965).

Table 9. *Positional and thermal parameters for the non-group atoms of* (7)

	x	y	z	B(Å^2)		x	y	z	B(Å^2)
Pd	0·33343 (7)	0·30079 (8)	0·15335 (3)	1·64 (6)	C(4)	0·5351 (9)	0·1719 (11)	0·1514 (4)	2·6 (3)
S	0·3079 (2)	0·4895 (3)	0·19805 (11)	2·89 (9)	C(5)	0·1720 (8)	0·4286 (11)	0·0898 (4)	2·2 (3)
O(SOL)	0·1170 (6)	0·3935 (8)	0·3467 (2)	3·2 (2)	C(6)	0·0675 (9)	0·4494 (12)	0·0585 (4)	3·7 (3)
N(SCN)	0·2373 (8)	0·3704 (11)	0·2761 (4)	4·9 (3)	C(7)	0·0944 (9)	0·2914 (11)	0·1473 (4)	3·3 (3)
N(1)	0·1804 (6)	0·3010 (8)	0·1178 (3)	1·5 (2)	C(8)	0·1089 (10)	0·1779 (12)	0·1824 (4)	4·2 (3)
N(2)	0·3605 (6)	0·1485 (8)	0·1107 (3)	1·5 (2)	C(9)	0·5536 (8)	0·4108 (11)	0·1716 (4)	2·8 (3)
N(3)	0·4930 (6)	0·2827 (8)	0·1781 (3)	1·6 (2)	C(10)	0·5452 (8)	0·4620 (11)	0·1239 (4)	2·8 (3)
C(SCN)	0·2673 (8)	0·4175 (11)	0·2442 (4)	2·6 (3)	C(11)	0·5111 (9)	0·2504 (12)	0·2290 (4)	2·6 (3)
C(1)	0·1782 (9)	0·1807 (11)	0·0860 (4)	2·6 (3)	C(12)	0·4445 (8)	0·1363 (12)	0·2438 (4)	2·9 (3)
C(2)	0·2813 (9)	0·1608 (11)	0·0691 (4)	2·6 (3)	C(SOL)	0·0759 (9)	0·2714 (13)	0·3629 (4)	3·8 (3)
C(3)	0·4736 (9)	0·1535 (11)	0·1044 (4)	2·6 (3)	B	0·6854 (12)	0·2991 (14)	0·3993 (5)	3·1 (4)

Table 10. *Derived parameters for the rigid-group atoms of* (7)

	x	y	z	B (Å^2)		x	y	z	B (Å^2)
*R*1C1	0·5626 (4)	0·3075 (6)	0·4122 (3)	1·1 (3)	*R*4C4	0·7512 (11)	0·0985 (15)	0·2717 (4)	1·7 (6)
*R*1C2	0·4780 (6)	0·2844 (6)	0·3776 (2)	1·2 (3)	*R*4C5	0·7985 (10)	0·2232 (15)	0·2829 (5)	1·7 (5)
*R*1C3	0·3742 (5)	0·2912 (7)	0·3880 (2)	2·1 (3)	*R*4C6	0·7758 (10)	0·2928 (11)	0·3221 (5)	−0·5 (11)
*R*1C4	0·3550 (4)	0·3210 (7)	0·4331 (3)	2·0 (3)	*R*2′C1	0·6943 (12)	−0·1737 (12)	0·3984 (7)	2·3 (6)
*R*1C5	0·4395 (6)	0·3440 (7)	0·4677 (2)	1·9 (3)	*R*2′C2	0·7150 (11)	−0·1038 (17)	0·4402 (5)	2·2 (6)
*R*1C6	0·5433 (5)	0·3373 (7)	0·4573 (2)	1·1 (3)	*R*2′C3	0·7151 (11)	0·0369 (17)	0·4404 (4)	1·6 (6)
*R*2C1	0·7101 (11)	0·4769 (11)	0·4000 (6)	0·8 (5)	*R*2′C4	0·6945 (11)	0·1077 (12)	0·3988 (6)	1·9 (6)
*R*2C2	0·7560 (11)	0·5448 (17)	0·4396 (4)	2·0 (6)	*R*2′C5	0·6738 (11)	0·0379 (18)	0·3570 (4)	1·8 (6)
*R*2C3	0·7612 (11)	0·6853 (17)	0·4398 (5)	1·5 (6)	*R*2′C6	0·6737 (11)	−0·1028 (18)	0·3568 (5)	1·6 (6)
*R*2C4	0·7205 (12)	0·7580 (11)	0·4004 (6)	1·9 (6)	*R*3′C1	0·7827 (11)	0·3475 (18)	0·4376 (5)	1·4 (6)
*R*2C5	0·6746 (11)	0·6902 (16)	0·3608 (5)	2·1 (6)	*R*3′C2	0·8771 (14)	0·2805 (12)	0·4529 (6)	2·4 (12)
*R*2C6	0·6695 (10)	0·5496 (16)	0·3606 (4)	1·5 (5)	*R*3′C3	0·9585 (10)	0·3480 (17)	0·4803 (5)	1·3 (5)
*R*3C1	0·7664 (11)	0·2257 (15)	0·4400 (5)	0·4 (5)	*R*3′C4	0·9455 (10)	0·4825 (17)	0·4925 (5)	3·1 (6)
*R*3C2	0·7284 (8)	0·1134 (16)	0·4616 (5)	1·1 (5)	*R*3′C5	0·8511 (13)	0·5496 (12)	0·4772 (5)	1·7 (6)
*R*3C3	0·7985 (12)	0·0303 (12)	0·4895 (5)	1·9 (5)	*R*3′C6	0·7697 (9)	0·4820 (18)	0·4497 (5)	1·4 (6)
*R*3C4	0·9066 (11)	0·0595 (14)	0·4958 (5)	3·7 (7)	*R*4′C1	0·7071 (12)	0·3513 (15)	0·3496 (4)	0·8 (5)
*R*3C5	0·9446 (8)	0·1719 (15)	0·4742 (6)	1·0 (5)	*R*4′C2	0·6496 (9)	0·4655 (15)	0·3336 (5)	1·4 (6)
*R*3C6	0·8745 (12)	0·2550 (13)	0·4464 (5)	1·2 (9)	*R*4′C3	0·6731 (10)	0·5317 (13)	0·2938 (5)	1·4 (5)
*R*4C1	0·7057 (11)	0·2376 (14)	0·3502 (4)	0·5 (5)	*R*4′C4	0·7541 (12)	0·4838 (16)	0·2701 (4)	1·6 (5)
*R*4C2	0·6585 (10)	0·1129 (15)	0·3390 (5)	1·1 (6)	*R*4′C5	0·8115 (10)	0·3697 (17)	0·2861 (5)	1·4 (5)
*R*4C3	0·6812 (10)	0·0434 (12)	0·2997 (5)	1·5 (5)	*R*4′C6	0·7880 (12)	0·3034 (13)	0·3259 (6)	3·2 (17)

Rigid-group parameters

Group	x_c^*	y_c	z_c	δ†	ε	η
Ring 1	0·4588 (4)	0·3142 (4)	0·42265 (18)	−1·622 (4)	2·796 (4)	−1·335 (4)
Ring 2	0·7153 (6)	0·6175 (11)	0·4002 (4)	1·53 (2)	2·040 (8)	0·0 (2)
Ring 3	0·8365 (8)	0·1426 (10)	0·4679 (3)	−0·920 (9)	2·855 (9)	0·547 (9)
Ring 4	0·7285 (7)	0·1681 (10)	0·3109 (3)	−0·693 (9)	2·855 (8)	−1·077 (8)
Ring 2′	0·6944 (6)	−0·0330 (12)	0·3986 (4)	1·55 (5)	1·789 (8)	0·02 (5)
Ring 3′	0·8641 (7)	0·4150 (12)	0·4650 (3)	0·596 (10)	−3·107 (9)	0·497 (9)
Ring 4′	0·7306 (7)	0·4176 (10)	0·3099 (3)	−2·314 (9)	2·954 (9)	−2·084 (9)

* x_c, y_c, and z_c are the fractional coordinates of the origin of the rigid group.
† The rigid-group orientation angles δ, ε, and η (radians) have been defined previously (La Placa & Ibers, 1965).

at the origin). The geometry of the anion is rather poorly determined, and the B–C distances vary over 0·3 Å (*ca* 15 e.s.d.'s). The coordinates of the single, average B atom are only approximate. There are, however, no problems with the isotropic refinement of the cation in $P2_1/n$, and none of the atomic B's is unusually large. An attempt to refine the structure in $P2_1$ was entirely unsuccessful. It may be that the structure is partially ordered.

A final problem concerned the high correlations between some of the atomic temperature factors of the groups, especially the B's of $R3C6$ and $R3'C2$, and of $R4C6$ and $R4'C6$; this correlation presumably explains the negative B for $R4C6$. Had this structure

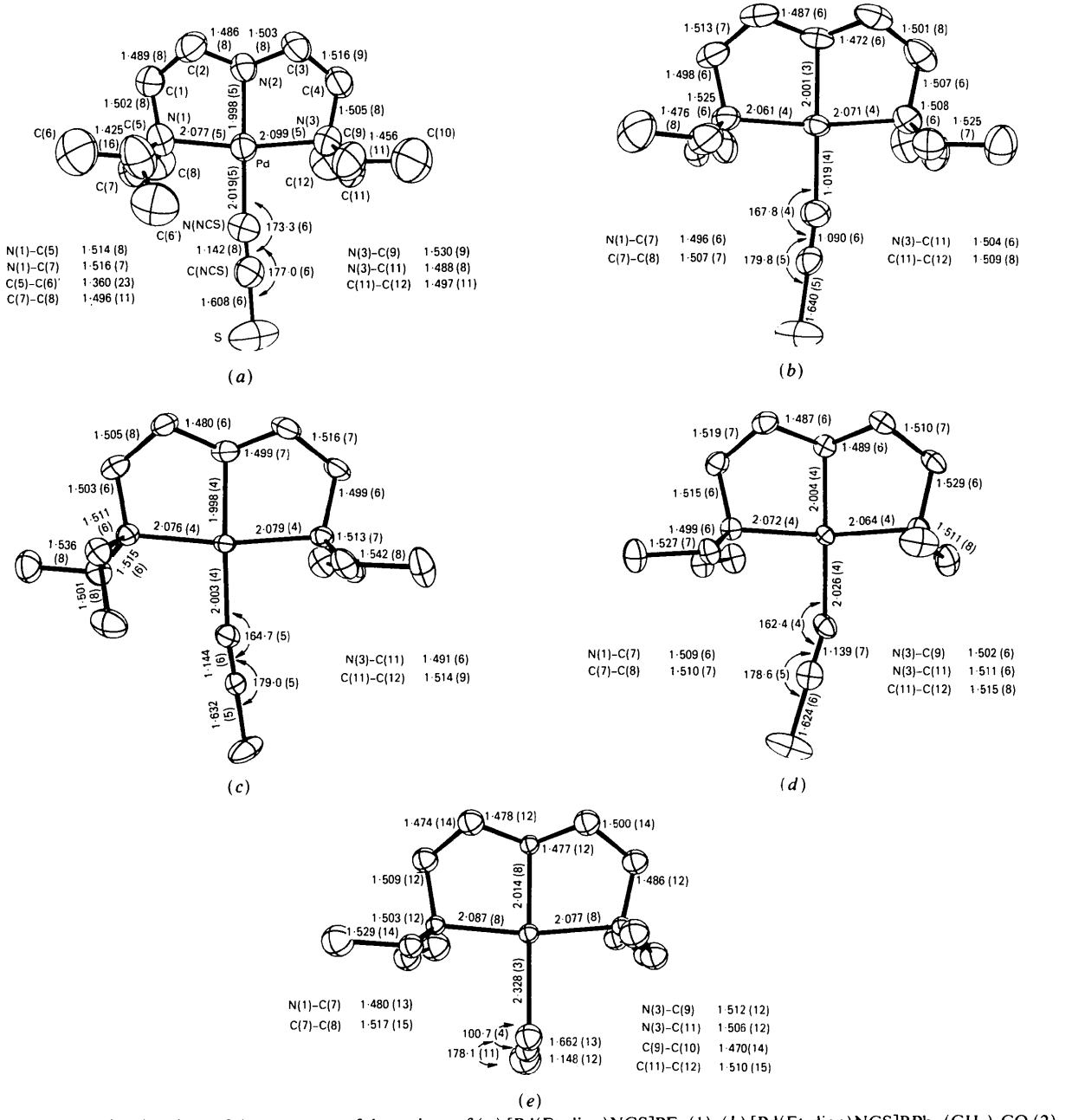

Fig. 1. Perspective drawings of the structures of the cations of (*a*) [Pd(Et_4dien)NCS]PF_6 (1), (*b*) [Pd(Et_4dien)NCS]BPh_4.$(CH_3)_2CO$ (2), (*c*) [Pd(Et_4dien)NCS]BPh_4 (3), (*d*) [Pd(Et_4dien)NCS]BPh_4.CH_2BrCl (5), and (*e*) [Pd(Et_4dien)SCN]BPh_4.CH_3OH (7). The atom-numbering scheme, which is the same for the five cations, and some bond lengths (Å) and angles (°) are shown. The cations have been drawn to the same scale and from the same perspective so that the sizes of the thermal ellipsoids may be compared. In these and the following drawings the shapes of the atoms correspond to 50% contours of thermal motion, and H atoms have been omitted for the sake of clarity.

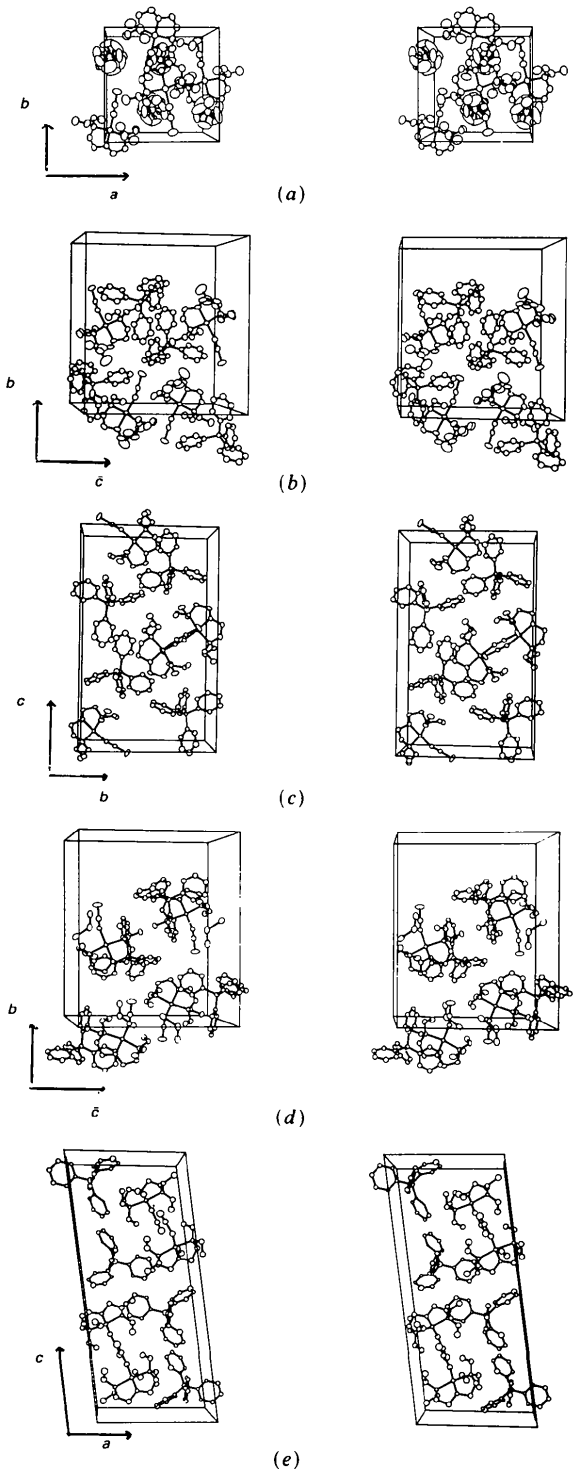

Fig. 2. Stereoscopic drawings of the contents of the unit cells of the five crystal structures reported in this paper. All five unit cells have been drawn to the same scale. (*a*) [Pd(Et$_4$dien)NCS]PF$_6$ (1), (*b*) [Pd(Et$_4$dien)NCS]BPh$_4$.-(CH$_3$)$_2$CO (2), (*c*) [Pd(Et$_4$dien)NCS]BPh$_4$ (3), (*d*) [Pd-(Et$_4$dien)NCS]BPh$_4$.CH$_2$BrCl (5), (*e*) [Pd(Et$_4$dien)SCN]-BPh$_4$.CH$_3$OH (7) (drawn as it might appear in $P2_1$; also, the isotropic B for R4C6 has been reset to 0·25).

Table 11. *Some results of the rigid-body thermal-motion analyses of the atoms* Pd, N(1), N(2), N(3), C(1), C(2), C(3), *and* C(4) *of the cation*

Structure designation*	(1)	(2)	(3)	(5)
Temperature (K)	296	143	150	150
T^{11} ($\times10^{-3}$ Å^2)†	51	27	17	21
T^{22} ($\times10^{-3}$ Å^2)	43	42	24	20
T^{33} ($\times10^{-3}$ Å^2)	50	35	22	15
L^{11} (deg^2)	11	6	6	6
L^{22} (deg^2)	24	9	9	9
L^{33} (deg^2)	10	11	6	5
R‡	0·012	0·022	0·026	0·032
Δ§	5×10^{-4}	4×10^{-4}	4×10^{-4}	4×10^{-4}

* See Table 1.

† Principal components of **T** and **L** are given with respect to a Cartesian coordinate system nearly centered on the Pd atom with **x** approximately parallel to Pd-N(2) and **y** approximately parallel to N(1)-N(3). Errors in T^{ii} and L^{ii} are about 1×10^{-3} Å^2 and 4 deg^2, respectively.

‡ $R=\{\sum[w(U_o^{ij}-U_c^{ij})]^2/\sum[wU_o^{ij}]^2\}^{1/2}$.

§ $\Delta=\{\sum[w(U_o^{ij}-U_c^{ij})]^2/\sum w^2\}^{1/2}$.

not contained the only S-bonded cation we were able to isolate, we might not have pursued it as vigorously.

Thermal-motion analyses

The anisotropic thermal parameters of the atoms forming the most rigid part of the cations, *i.e.* the Pd atom and the backbone atoms of the triamine ligand, were analyzed in terms of the Schomaker-Trueblood rigid-body **TLS** model using Trueblood's (1978) program *THMI*. The fits (see Table 11) are excellent. In lieu of listing all 20 independent tensor components for each of the four structures, we are presenting only the principal components of **T** and **L** as referred to coordinate systems based on the inertia tensors of the cation fragments. Differences in these systems between the four structures are very small.

Spectra

Infrared spectra were recorded at room temperature on a Perkin-Elmer 621 spectrophotometer as Nujol mulls and were calibrated with a polystyrene film. Frequencies of the C-N asymmetric stretches are given in Table 1.

Discussion

This study confirms the idea that the relative stability in the solid state of the N- and S-bonded isomers of [Pd(Et$_4$dien)CNS]$^+$ may depend on crystal packing, but refutes the suggestion (BGL, 1969; Lauer, Peterkin, Burmeister, Johnson & Lim, 1972) that BPh_4^- salts will always isomerize in a period of weeks to the S-bonded isomer; several of the crystal forms of the BPh_4^- salt containing the N-bonded isomer are perfectly stable over a period of months. The observation that the preponderance of crystal forms contains the N-bonded cation suggests, in agreement with the

solution-phase evidence (BGL, 1969; Basolo, Baddley & Weidenbaum, 1966), that it is the more stable isomer. On the other hand, the existence of crystal forms of both isomers demonstrates the crystal-packing effect and is a clear indication that the energies of the cations differ by less than about 10 kJ mol^{-1}. This estimate is very similar to those given previously (Hewkin & Poë, 1967; Mares, Palmer & Kelm, 1982).

The study of solid-state transitions of the BPh_4^- salt is greatly complicated by the discovery of the existence of multiple crystal forms. As a consequence, reactions must be carried out on material identified as belonging to a specific solid phase. The material reported by Burmeister, Gysling & Lim (1969) to undergo an N- to S-bonded isomerization was a powder of the BPh_4^- salt, precipitated by pouring 10 ml of a DMF solution into 400 ml of ice water. While the published infrared spectrum does indicate that this material contains mostly N-bonded isomer, there is no way of determining whether or not it is a single phase. The original paper reported nearly complete isomerization to S-bonded material, as judged from infrared spectra, but in several attempts to repeat the work we could obtain no more than a partial conversion. It may be that small differences in our procedure from that of BGL (1969) gave powdery BPh_4^- salt with a different mix of phases. In later work (Lauer, Peterkin, Burmeister, Johnson & Lim, 1972) the reaction was reported to go only 75% of the way to completion. None of the single crystals we have studied appears to undergo the reported transition. Given the propensity of the BPh_4^- salt to incorporate solvent, and the abundance of water present during precipitation, we wonder if there is any chance that the isomerizing material is a hydrate. It is also possible that the isomerization occurs primarily at the surfaces and so is extremely slow for single crystals.

Only one crystal form (6) of those we studied showed a time-dependent change in the infrared spectrum (see Fig. 3), and this change is not readily interpreted. The two bands at 2131 and 2113 cm^{-1} are both in the range expected for the pseudo-asymmetric C–N stretch of the S-bonded SCN^- ligand (Bailey, Kozak, Michelsen & Mills, 1971). The latter has the same frequency and shape as the band reported for the S-bonded isomer (BGL, 1969), and it is this band which grows in intensity at the expense of the one at 2131 cm^{-1}. Unfortunately, we were unable to study this crystal form in detail, and can only draw inferences about it from the low-temperature study of what is presumably a related structure (7). Since crystals of the two forms [(6) and (7)] were grown in the same way and have similar morphologies, we expect that (7) is simply the low-temperature form of (6). If so, it is unlikely that there are large differences in the overall packing or in the bonding of the SCN^- ligand, since any such change would probably shatter the crystal during cooling. The unit cell of (7) is about half as big as that of (6), and in (7) there is a CH_3OH molecule hydrogen-bonded to the N(SCN) atom (see below). It may be that the methanol is slowly lost at room temperature while the crystal structure is rearranged and the C–N stretch is shifted to a slightly lower frequency. There is, however, no obvious relationship between the two unit cells.

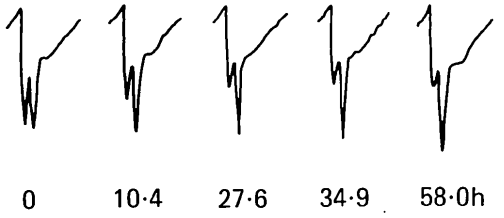

Fig. 3. The C–N stretching bands (2131 and 2113 cm^{-1}) of a Nujol mull of the room-temperature form of $[Pd(Et_4dien)SCN]BPh_4$ [(6); CH_3OH solvate?] as a function of time.

The abundance of crystal forms of the $[Pd(Et_4dien)CNS]^+$ ion makes it possible to determine whether there are any motifs which dominate its packing. An examination of unit-cell stereopairs (see Fig. 2) suggests a tendency for the Pd atom of one cation to interact, albeit very weakly, with the free end of the NCS^- or SCN^- ligand of another. As a result, most of the structures contain chains or stacks of approximately aligned Pd–N or Pd–S vectors. These interactions are particularly apparent in the unsolvated BPh_4^- salt (3) containing the N-bonded isomer and in the CH_3OH-solvated salt (7) containing the S-bonded isomer [see Fig. 2(*c*) and (*e*)]. In both structures there are infinite columns of interacting cations related by crystallographic 2_1 axes; in the former the Pd···S distances within the stack are 3·970 (2) and 5·627 (2) Å, while in the latter the Pd···N(SCN) distances are 4·875 (10) and 6·123 (12) Å. In the CH_3OH solvate the hydroxyl group also forms a hydrogen-bonded bridge between the N(2) and N(SCN) atoms of pairs of cations; distances from O(SOL) to these atoms are 2·817 (11) and 2·728 (13) Å respectively. It has been suggested (Burmeister, 1975) that protic solvents stabilize the S-bonded isomer by hydrogen bonding to the free N atom. In the PF_6^- (1) salt (Fig. 2*a*) the interacting cations also form chains, but in this case the 2_1 axes relating the constituent cations are more or less parallel, rather than perpendicular, to the Pd–CNS grouping. The Pd···S distance is 4·407 (2) Å. In the $(CH_3)_2CO$ (2) and CH_2BrCl (5) solvates, the solvent molecules appear to interfere with any such interactions. In neither structure is there any Pd···S or Pd···N distance shorter than 6·0 Å, and most are several Å longer. The acetone molecule is hydrogen bonded to H(N2) [the O(SOL)···N(2) distance is 2·875 (5) Å], an interaction which undoubtedly accounts for the resistance of these crystals to loss of solvent.

In comparing these five crystal structures, it would be useful to estimate the relative 'tightness of packing' of the cation in its different environments. Densities are not helpful since no two of the salts have the same chemical composition. Average non-bonded contact distances could be compared, but we suggest that thermal-motion parameters, while more susceptible to systematic error (such as unrecognized disorder or uncorrected absorption effects), contain the desired information in a more accessible form. The looser the packing of a molecule or ion, the larger its thermal-motion parameters. For rigid groups of atoms the anisotropic thermal parameters can be analyzed in terms of the Schomaker–Trueblood rigid-body model; partial results are given in Table 11 for the most rigid fragments of the cations of the four structures for which β's were refined. In order to include the non-rigid parts of the cations and the isotropically refined structure we have also plotted (see Fig. 4) the equivalent isotropic B's $[\frac{4}{3}\mathrm{Tr}(\boldsymbol{\beta}\,.\,\mathbf{G})]$ for the corresponding atoms of the five structures. The two ways of presenting the data lead to the same conclusions. Of the four structures studied at low temperature (137–150 K) three are remarkably similar; the thermal-motion parameters for the acetone solvate (2), however, are much larger. The thermal motion of the cation in the PF_6^- and BPh_4^- salts can also be compared since the T and L tensors expand approximately linearly with temperature. After this correction is made, the packing in the PF_6^- salt seems to be tighter than in the acetone solvate and similar to that found in the other three structures. It is interesting that crystal stability and tightness of packing, at least as measured in this way, do not appear correlated. It should be noted that the isotropic B's for the structure containing the S-bonded cations (7) are likely to be systematically in error owing to the very limited data set, but that the absence of higher-angle data is more likely to lead to over- rather than underestimation of thermal motion (Brock & Dunitz, 1982).

The geometry of the N-bonded cation, determined in four structures, is very precisely determined. Average bond lengths and angles are given in Fig. 5 along with the e.s.d.'s describing the widths of the distribution; the e.s.d.'s of the individual dimensions (*i.e.* of the means) are smaller by factors of $\sqrt{4}$, $\sqrt{8}$, or $\sqrt{16}$. No corrections have been made for thermal motion, hence the short ethyl C–C bond length and relatively large e.s.d. Other dimensions of the cation are less affected by thermal motion, which differs considerably between the structures, so that the other e.s.d.'s are in general smaller. They average about 0·01 Å and 1°. Neither the averages nor the e.s.d.'s for most of the dimensions change appreciably if the data for the S-bonded cation are included.

One bond length and two angle distributions stand out as being particularly wide. The N–C bond of the NCS^- ligand is short for the acetone solvate (1·090 Å); the average for the other three structures is 1·142 Å with an e.s.d. of 0·003 Å. Although there were absolutely no indications of problems with the refinement of this structure, we must wonder if the N(NCS) and C(NCS) atoms might be slightly misplaced. The variation of the Pd–N–C(NCS) bond angle, however, is not surprising. Little energy is lost in deforming it while the corresponding change in the position of the S atoms (nearly 0·5 Å for a 10° bend) may substantially improve the intra- and interionic interactions. Consequently, this angle may

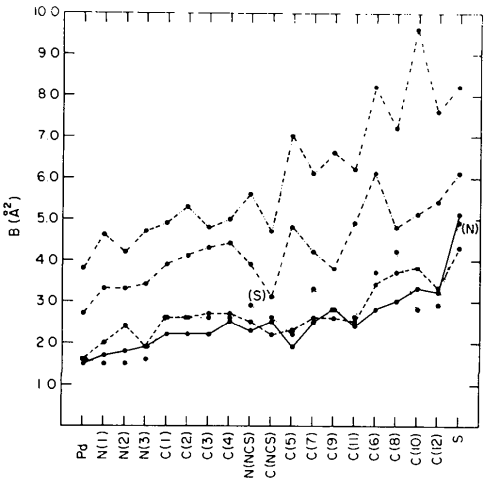

Fig. 4. Equivalent isotropic temperature factors $[B_{eq} = \frac{4}{3}\mathrm{Tr}(\boldsymbol{\beta}\,.\,\mathbf{G})]$ for the atoms of the $[Pd(Et_4dien)CNS]^+$ cation as observed in the PF_6^- salt (1) at 296 K (– · · –); the BPh_4^- salt, $(CH_3)_2CO$ solvate (2) at 143 K (– · –); the BPh_4^- salt (3) at 150 K (– – –); and the BPh_4^- salt, CH_2BrCl solvate (5) at 150 K (——). B's for the BPh_4^- salt, CH_3OH solvate (7) at 137 K (· · · ·) are also shown. The atoms are approximately ordered from left to right according to their increasing distance from the center of mass.

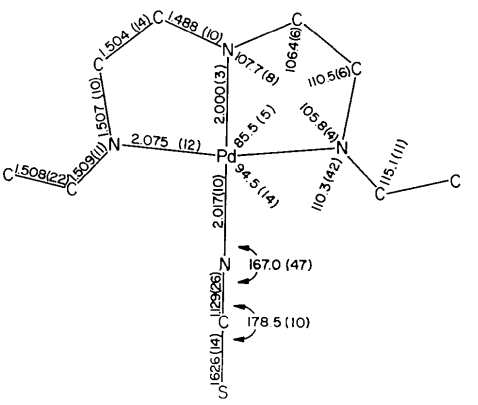

Fig. 5. Diagram of $[Pd(Et_4dien)NCS]^+$ showing distances (Å) and angles (°) averaged over the two halves of the cation and the four structure determinations. The numbers in parentheses are the estimated σ's that measure the widths of the distributions; the e.s.d.'s of the means can be obtained by dividing these numbers by the square root of the number of values in the respective samples.

Table 12. Pd-N-C(*ethyl*) *angles* (°)

Structure* designation	Pd-N(1)-C(5)	Pd-N(1)-C(7)	Pd-N(3)-C(9)	Pd-N(3)-C(11)
(1)	107·3 (4)	115·8 (4)	106·4 (4)	113·0 (4)
(2)	104·3 (3)	115·2 (3)	105·1 (3)	114·0 (3)
(3)	110·3 (3)	111·8 (3)	105·2 (3)	115·3 (3)
(5)	104·7 (3)	114·4 (3)	110·0 (3)	112·3 (3)
(7)	105·5 (6)	115·3 (7)	112·1 (6)	112·2 (6)

* See Table 1.

be expected to depend on crystal packing. Finally, a histogram (Fig. 6) of the Pd-N-C(ethyl) angles suggests that this wide distribution is multi-, probably tri-, modal. The largest angles (see Table 12 and Fig. 1) are associated with the ethyl groups containing C(7) and C(11) that are 'tucked under' the triamine ligand and may interfere with the Pd and C(1) or C(4) atoms. The smallest angles are those of the ethyl groups containing C(5) and C(9) that extend out to either side (see, *e.g.*, Fig. 1*b*), while the angles of the ethyl groups that take other positions, such as C(5)-C(6) of the unsolvated BPh_4^- salt (Fig. 1*c*), have intermediate values.

Interference of the ethyl groups of the 1,1,7,7-tetraethyldiethylenetriamine ligand with the CNS^- ligand has been cited as destabilizing the S-bonded relative to the N-bonded isomer (Basolo, Baddley & Burmeister, 1964; Hewkin & Poë, 1967). The conformation found for the S-bonded isomer (Fig. 1*e*) is probably the most favorable possible; rotation about the Pd-S or $N-C_2H_5$ bonds would lead to very unfavorable interactions. It may be, however, that this one conformation is not so much higher in energy than the average conformation of the N-bonded isomer. In solution entropy differences may favor the N-bonded isomer with its greater conformational freedom; however, this consideration is not important if the stabilities of the two isomers are being compared in the solid state where all motion is highly restricted.

To summarize, this study shows the supposed counterion control of the linkage isomerism in $[Pd(Et_4dien)CNS]^+$ to be a false generalization drawn from an isolated example of a crystal-packing effect. The $B(C_6H_5)_4^-$ ion *per se* does not preferentially stabilize the Pd-SCN isomer as claimed, although there may be crystal modifications of the $B(C_6H_5)_4^-$ salt for which the Pd-SCN isomer happens to be favored. Furthermore, the explanation for the supposed counterion control, that 'the more nearly spherical

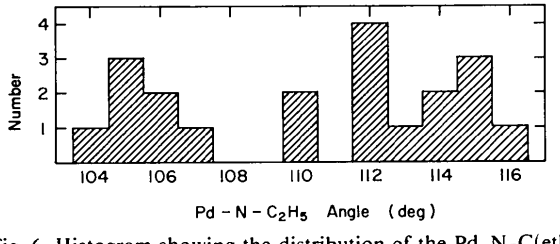

Fig. 6. Histogram showing the distribution of the Pd-N-C(ethyl) angles in the five structures of the $[Pd(Et_4dien)CNS]^+$ cation.

$[Pd(Et_4dien)SCN]^+$ ion would be expected to pack more efficiently with the large, spherically symmetrical $[B(C_6H_5)_4]^-$ than would the N-bonded isomer with its linear Pd-NCS linkage sticking out like a sore thumb' (Burmeister, 1975), demonstrates the danger in making generalizations about solid-state effects in the absence of crystal structure data. The crystal packing in the two types of salts is not dissimilar; the dominant motif, the alignment of the Pd-NCS vectors (probably a dipole interaction), is seen in both the PF_6^- and several of the $B(C_6H_5)_4^-$ salts. In fact, interaction between the CNS^- ligands is actually strongest in the *M*-SCN structure of the $B(C_6H_5)_4^-$ salt, the reverse of Burmeister's (1975) prediction. The density, or 'efficiency', of packing, at least as measured by a thermal-motion criterion, is not correlated with the isomer or anion type either. Finally, even the smallest structural details in the four Pd-NCS structures are nearly the same. The Pd-N-C(NCS) angle does vary slightly with crystal packing, and the ethyl groups can adopt one of several well defined conformations; otherwise, the cation geometry is remarkably constant. Thus we conclude that the most stable form of the cationic complex in solution also predominates in the solid state, regardless of the identity of the non-coordinating anion. The structure of $[Pd(Et_4dien)SCN][B(C_6H_5)_4]$ is the exception that proves this important principle. This one Pd-SCN isomer is stabilized in the solid state by special interactions, the formation of H-bonded bridges with included solvent, that do not depend in any direct way on the nature of the anion.

This research was partially supported by a Research Corporation Grant to TGA. JLH thanks the Ashland Oil Corporation for an Undergraduate Summer Fellowship.

References

BAILEY, R. A., KOZAK, S. L., MICHELSEN, T. W. & MILLS, W. N. (1971). *Coord. Chem. Rev.* **6**, 407-445.

BASOLO, F., BADDLEY, W. H. & BURMEISTER, J. L. (1964). *Inorg. Chem.* **3**, 1202-1203.

BASOLO, F., BADDLEY, W. H. & WEIDENBAUM, K. J. (1966). *J. Am. Chem. Soc.* **88**, 1576-1578.

BROCK, C. P. & ATTIG, T. G. (1980). *J. Am. Chem. Soc.* **102**, 1319-1326.

BROCK, C. P. & DUNITZ, J. D. (1982). *Acta Cryst.* B**38**, 2218-2228.

BROCK, C. P. & WEBSTER, D. F. (1976). *Acta Cryst.* B**32**, 2089-2094.

BURMEISTER, J. L. (1975). *The Chemistry and Biochemistry of Thiocyanic Acid and Its Derivatives*, edited by A. A. NEWMAN, pp. 68-130. London: Academic Press.

BURMEISTER, J. L., GYSLING, H. J. & LIM, J. C. (1969). *J. Am. Chem. Soc.* **91**, 44-47.

BURMEISTER, J. L., HASSEL, R. L., JOHNSON, K. A. & LIM, J. C. (1974). *Inorg. Chim. Acta*, **9**, 23-28.

HEWKIN, D. J. & POË, A. J. (1967). *J. Chem. Soc. A*, pp. 1884-1889.

LA PLACA, S. J. & IBERS, J. A. (1965). *Acta Cryst.* **18**, 511-519.

LAUER, J. L., PETERKIN, M. E., BURMEISTER, J. L., JOHNSON, K. A. & LIM, J. C. (1972). *Inorg. Chem.* **11**, 907-909.

MACDOUGALL, J. J., NELSON, J. H., FULTZ, W. C., BURMEISTER, J. L., HOLT, E. M. & ALCOCK, N. W. (1982). *Inorg. Chim. Acta*, **63**, 75-83.
MARES, M., PALMER, D. A. & KELM, H. (1982). *Inorg. Chim. Acta*, **60**, 123-127.
NELSON, J. H., MACDOUGALL, J. J., ALCOCK, N. W. & MATHEY, F. (1982). *Inorg. Chem.* **21**, 1200-1204.
NORBURY, A. H. (1975). *Adv. Inorg. Chem. Radiochem.* **17**, 231-386.
TRUEBLOOD, K. N. (1978). *Acta Cryst.* A**34**, 950-954.

Acta Cryst. (1984). B**40**, 606-612

Structural and Vibrational Analysis of Nonacarbonyltri-μ-hydrido-μ_3-methylidyne-*triangulo*-triosmium. X-ray and Neutron Diffraction Studies*

BY A. G. ORPEN†
Department of Inorganic Chemistry, The University, Bristol BS8 1TS, England
AND T. F. KOETZLE
Department of Chemistry, Brookhaven National Laboratory, Upton, New York 11973, *USA*

(*Received* 16 *January* 1984; *accepted* 2 *May* 1984)

Abstract

X-ray and neutron diffraction studies on the complex $Os_3(\mu\text{-}H)_3(\mu_3\text{-}CH)(CO)_9$ have been carried out at 200 and 11K respectively. The structure is triclinic, space group $P\bar{1}$, with $a = 9{\cdot}399\,(3)$, $b = 11{\cdot}665\,(4)$, $c = 15{\cdot}651\,(7)$ Å, $\alpha = 112{\cdot}32\,(3)$, $\beta = 90{\cdot}11\,(3)$, $\gamma = 97{\cdot}80\,(3)°$, $R(F) = 0{\cdot}044$ for 4121 observed reflections at 200 K, and $a = 9{\cdot}295\,(2)$, $b = 11{\cdot}457\,(3)$, $c = 15{\cdot}622\,(4)$ Å, $\alpha = 111{\cdot}66\,(2)$, $\beta = 90{\cdot}32\,(2)$, $\gamma = 96{\cdot}93\,(2)°$, $R(F) = 0{\cdot}022$ for 4962 observed reflections at 11 K. The structure contains two crystallographically independent molecules, each of which shows $3m$ (C_{3v}) symmetry to within experimental error. All carbonyl ligands are terminal and near linear, the hydride H atoms bridge the Os–Os vectors symmetrically, and the Os_3 triangle is bridged by a methylidyne group. Molecular geometric parameters averaged over $3m$ symmetry and both molecules, at 11 K, are: bond lengths Os–Os 2·893 (2), Os–H 1·834 (3), Os–C(H) 2·101 (2), Os–C(*trans* to H) 1·911 (2), Os–C(*trans* to C) 1·964 (2), C–O 1·141 (1), and C–H 1·086 (2) Å; bond angles Os–H–Os 104·2 (2), Os–C–Os 87·0 (1), and Os–C–O 178·0 (3)°. The neutron data provide a measure of the vibrational behaviour of the H atoms and allow estimation of the frequencies of the internal hydrogen vibrational modes. The hydride hydrogen frequencies calculated assuming the modes to be harmonic and uncoupled are 1395 (30), 1332 (45) and 625 (5) cm^{-1} for the symmetric and antisymmetric stretch and deformation vibrations, respectively. The methylidyne hydrogen ν_{C-H} and δ_{C-H} frequencies are calculated to be 2870 (150) and 867 (20) cm^{-1}. The Fourier transform IR spectrum of $Os_3(\mu\text{-}H)_3(\mu_3\text{-}CH)(CO)_9$ was measured at low temperature giving frequencies in agreement with those calculated from the diffraction data.

Introduction

Organometallic cluster complexes containing a μ_3-alkylidyne ligand have been amongst the most intensively studied of such molecules. These studies have elucidated both the geometrical structure of representative examples of these species [*e.g.* $Co_3(CO)_9(\mu_3\text{-}CCH_3)$ (Sutton & Dahl, 1967)] and their reactivities. In addition, the electronic structure of such complexes has been examined by experimental methods [photoelectron spectroscopy (Sherwood & Hall, 1982; DeKock, Wong & Fehlner, 1982, and references therein) and diffraction methods (Leung, Coppens, McMullan & Koetzle, 1981; Leung, Holladay & Coppens, 1981)] and analysed theoretically (Sherwood & Hall, 1982; DeKock, Wong & Fehlner, 1982, and references therein). The interest in such molecules has been stimulated by the possibility that the observed μ_3-C*R* bonding mode may be a good model for the binding of such organic fragments to metal surfaces (*e.g.* Muetterties, Rhodin, Band, Brucker & Pretzer, 1979). We report here X-ray and neutron single-crystal diffraction studies on $Os_3(\mu\text{-}H)_3(\mu_3\text{-}CH)(CO)_9$ at 200 and 11 K respectively. The synthesis of this compound by Calvert & Shapley (1977) beautifully illustrates the reasons for the interest in the chemistry of cluster complexes as models for the chemistry of metal surfaces. Thus at various stages C–H, Os–H and Os–C bond formation and cleavage mediated by the cluster were observed, and at least three binding modes for simple C_1 hydrocarbon fragments were identified (*i.e.* μ-CH_3, μ-CH_2 and μ_3-CH). Such processes are key ones in the reactions of hydrocarbons with surface metal atoms. The low temperature at which neutron data were collected has enabled very precise characterization

* Carried out, in part, under contract with the US Department of Energy, Office of Basic Energy Sciences.
† Author to whom correspondence should be addressed.

0108-7681/84/060606-07$01.50